

## Intrinsic AGN Absorption Lines

Any gaseous material along our line of sight to distant quasars or, more generally, active galactic nuclei (AGNs) will absorb light according to the amounts and range of ions present. Strong absorption lines are common in rest-frame UV spectra of AGNs due to a variety of resonant transitions, for example the HI Lyman series lines (most notably Ly $\alpha$   $\lambda$ 1216) and high-ionization doublets like CIV  $\lambda\lambda$ 1549,1551. The lines are called *intrinsic* if the absorbing gas is physically related to the AGN, e.g. if the absorber resides broadly within the radius of the AGN's surrounding "host" galaxy. Intrinsic absorption lines are thus valuable probes of the kinematics, physical conditions and elemental abundances in the gas near AGNs.

Studies of intrinsic absorbers have historically emphasized quasar broad absorption lines (BALs), which clearly identify energetic outflows from the central engines. Today we recognize a wider variety of intrinsic lines in a wider range of objects. For example, we now know that Seyfert 1 galaxies (the less luminous cousins of quasars) have intrinsic absorption. We also realize that intrinsic lines can form in a range of AGN environments — from the dynamic inner regions like the BALs, to the more quiescent outer host galaxies  $>10$  kpc away. One complicating factor is that most AGNs also have absorption lines due to unrelated gas or galaxies far from the AGN (see QUASARS: ABSORPTION LINES). Part of the effort, therefore, is to identify the intrinsic lines and locate their absorbing regions relative to the AGNs. Empirical line classifications are a good starting point for this work.

### Empirical Line Types

AGN absorption lines are usually classified according to the widths of their profiles. These classes separate the clearly intrinsic broad lines from the many others of uncertain origin. The main empirical classes are 1) the BALs, 2) the narrow absorption lines (NALs), and 3) the intermediate "mini-BALs."

Broad absorption lines (Fig. 1) are blueshifted relative to the AGN emission lines, implying outflow velocities from near  $0 \text{ km s}^{-1}$  to as much as  $\sim 60,000 \text{ km s}^{-1}$  ( $\sim 0.2c$ ). A representative line width is  $\sim 10,000 \text{ km s}^{-1}$ , although there is considerable diversity among BAL profiles. Velocity widths  $\gtrsim 3000 \text{ km s}^{-1}$  and blueshifted velocity extrema  $\gtrsim 5000 \text{ km s}^{-1}$  are usually considered minimum requirements for classification as a BAL. Some BALs have several distinct absorption troughs, while others are strictly "detached" from the emission lines — such that the absorption appears only at blueshifts exceeding several thousand  $\text{km s}^{-1}$ .

Narrow absorption lines (Fig. 2) have widths less than a few hundred  $\text{km s}^{-1}$ . NALs with absorption red-

shifts,  $z_a$ , within  $\pm 5000 \text{ km s}^{-1}$  of the emission redshift,  $z_e$ , are called "associated" (or  $z_a \approx z_e$ ) lines because of their likely physical connection to the AGN. In general, NALs can appear at redshifts from  $z_a \approx z_e$  to  $z_a \approx 0$ . Many of these systems are not related to the AGNs.

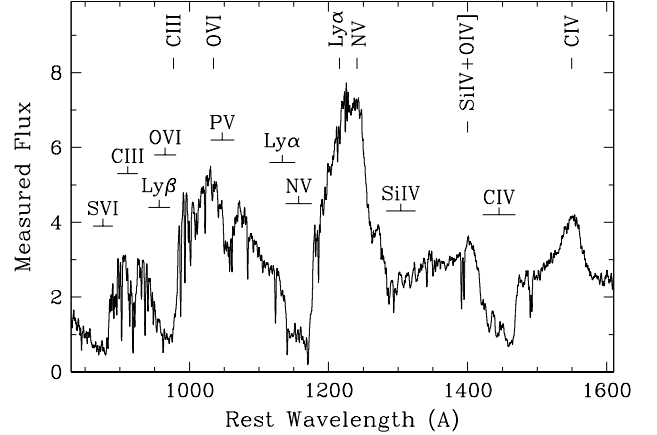


Figure 1. — Detached BALs in the quasar PG 1254+047. The BALs are labeled just above the spectrum. The wavelengths of prominent broad emission lines are marked across the top. The Flux has units  $10^{-15} \text{ ergs s}^{-1} \text{ cm}^{-2} \text{ \AA}^{-1}$ .

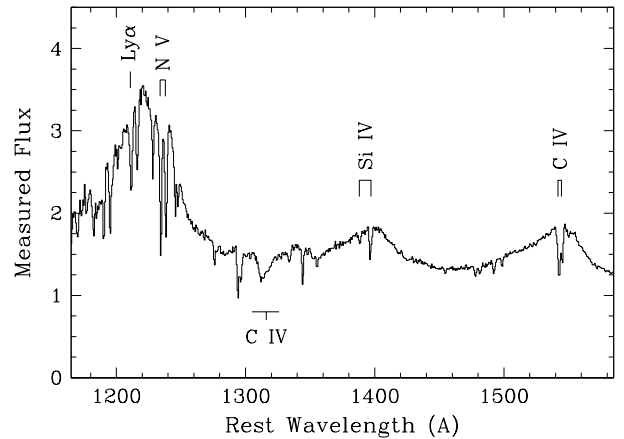


Figure 2. — Intrinsic absorption in the quasar PG 0935+417. A system of associated NALs is labeled above the spectrum, with open brackets showing the doublet separations. A mini-BAL due to CIV blueshifted by  $\sim 51,000 \text{ km s}^{-1}$  is labeled below. The Flux has units  $10^{-15} \text{ ergs s}^{-1} \text{ cm}^{-2} \text{ \AA}^{-1}$ .

Absorption lines with intermediate widths between the BALs and NALs are increasingly called mini-BALs (Fig. 2). Their strictly blueshifted profiles appear smooth and BAL-like in high resolution spectra, and their centroid velocities span the same range as the BAL troughs (from near  $0 \text{ km s}^{-1}$  to almost  $0.2c$ ). Mini-BALs evidently form in outflows similar to the BALs.

## Identifying Intrinsic NALs

The first evidence that some NALs are intrinsic came from statistical tendencies, namely, 1) quasar NALs appear with greater frequency near the emission-line redshift, and 2) the strengths of these  $z_a \approx z_e$  systems correlate with the quasars’ radio properties. The first tendency might be explained by external galaxies clustering around quasars, but the second clearly demonstrates a physical relationship to the quasars themselves.

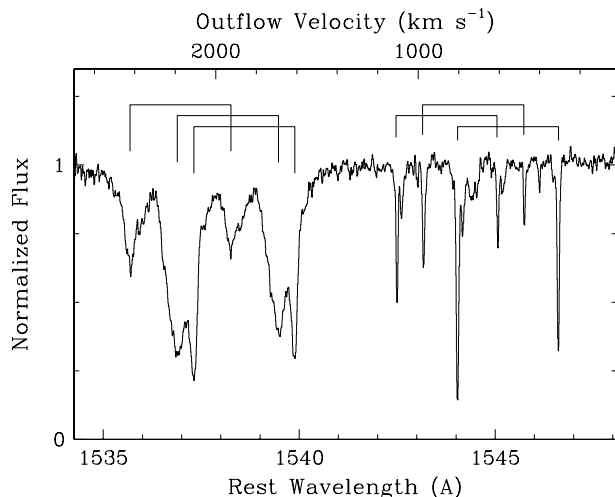


Figure 3. — High resolution blow-up of the CIV NALs in PG 0935+417, revealing multiple components (cf. Fig. 2). The open brackets mark the strongest doublet pairs. The outflow velocities are appropriate for the short-wavelength doublet members. The absorption complex at 1535–1540 Å is intrinsic based on the broad line profiles and doublet ratios that imply partial line-of-sight coverage.

Direct evidence for the intrinsic origin of specific NALs has come from spectroscopic indicators, such as 1) time-variable line strengths, 2) well-resolved line profiles that are smooth and broad compared to the thermal velocity, 3) multiplet ratios that imply partial coverage of the background light source(s), and 4) high space densities ( $\gtrsim 100 \text{ cm}^{-3}$ ) inferred from the presence of excited-state absorption lines. These properties signal intrinsic absorption because they are most easily understood in terms of the dense and dynamic environments near AGNs. Unrelated intervening absorbers — typically inter-galactic gas clouds or extended galactic halos — should generally be larger, more quiescent, and less ionized for a given gas density. The link between the first 3 properties and the near-quasar environment is further strengthened by the fact that they are common in BALs and mini-BALs. NALs with these characteristics probably also form in outflows; they have been measured at blueshifted (ejection) velocities from  $\sim 0$  to  $\sim 24,000 \text{ km s}^{-1}$  (e.g. Fig. 3).

## Global Covering Factors and the Ubiquity of Intrinsic Absorbers

All varieties of quasars and Seyfert 1 galaxies show some type of intrinsic absorption, but different objects favor different types of absorbers. For example, BALs and other high-velocity ( $\gtrsim 3000 \text{ km s}^{-1}$ ) intrinsic lines appear only in quasars and never in the Seyfert galaxies. BALs also tend to avoid quasars with strong radio emission, while associated NALs seem to favor them. Preferences like these are probably tied to the unique physical conditions, whereby different AGNs drive different types of outflows.

Intrinsic lines also do not appear in every individual spectrum. For example, BALs are detected in only  $\sim 12\%$  of quasars. The detection rate of associated (and so probably intrinsic) NALs in quasars is not well known, but it appears to be roughly similar to the BALs. Mini-BALs may be somewhat rarer than both BALs and associated NALs in quasars, but they can appear in either “radio-loud” or “radio-quiet” objects. Mini-BALs and intrinsic NALs are both common in Seyfert 1 galaxies, with at least one of these features appearing in 50–70% of the low-luminosity sources.

These detection rates (within object classes) depend on viewing angle effects and on the global covering factors of the absorbing gas. If the objects are randomly oriented, the absorption-line detection frequencies should approximately equal the average value of the global covering factor,  $Q \equiv \Omega/4\pi$ , where  $\Omega$  is the solid angle subtended by the absorber as seen from the central light source. In practice, the situation can be more complicated. For example, attenuation by BAL gas might bias quasar samples against the inclusion of sources with BALs. Thus the true global covering factor of BAL regions could be 20–30%, instead of the  $\sim 12\%$  implied by the detection rate. Nonetheless, the overall conclusion is that intrinsic absorbers are present in all AGNs, with global covering factors *similar* to the line detection frequencies in each type of object.

## Absorber Geometry

A consistent picture of the geometry has emerged in which the absorbing gas resides primarily near the equatorial plane of the AGN accretion disk (Fig. 4). In particular, spectropolarimetric observations show that the continuum light from BAL quasars is more polarized than non-BAL quasars. Also, the percent polarization is typically much greater inside BAL troughs compared to the adjacent continuum. These results are understood in terms of light scattering in the disk geometry. Quasars viewed close to edge-on exhibit BALs because our sight-line intersects the the absorbing gas. These objects are also more polarized because the direct (unpolarized) light through the BAL region is slightly

attenuated; thus the scattered (polarized) light makes a relatively larger contribution to their measured flux. BAL troughs have higher percent polarizations because the direct (unpolarized) light in the troughs is more attenuated than the continuum. Quasars without BALs, viewed from above or below the disk plane, have low polarizations because their direct (unpolarized) light dominates the measured flux.

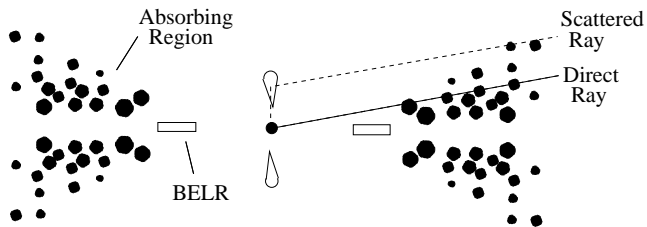


Figure 4. — Schematic absorber geometry. The dotted lines are representative light rays from the continuum source (central dot). The open rectangles mark the broad emission line region (BELR) near the accretion disk plane. The teardrop lobes above and below are putative scattering regions near the disk axis. Extended radio jets, when present, would lie along this axis.

This picture is also supported by observations showing that quasars with reddened spectra, presumably caused by dust near the disk plane, are more likely to have BALs and high polarizations. Similarly, studies of radio-loud quasars show that associated NALs are stronger and more common in sources with their radio jets aligned perpendicular to our line of sight (such that their unresolved inner disks are viewed nearly edge-on).

## Basic Physical Properties

### Kinematics

One surprising property of intrinsic absorbers is that none of them have changed velocity between observations that now span 10–20 yrs. In one well-studied case, distinct features in a quasar BAL show  $<30 \text{ km s}^{-1}$  of movement over 5 yrs in the quasar rest frame, implying an acceleration of  $<0.02 \text{ cm s}^{-2}$ . The outflow speeds of  $10,000\text{--}20,000 \text{ km s}^{-1}$  are therefore stable to  $\lesssim 0.2\%$  on this time scale.

Another general property is the kinematic complexity (e.g. Figs. 1–3). Many intrinsic absorbers have multiple distinct absorption troughs. Sometimes BALs, mini-BALs and/or NALs appear together in the same spectrum, either blended together or at different (non-overlapping) outflow velocities. The narrower lines, i.e. the NALs and mini-BALs, generally have small velocity dispersions compared to the outflow speeds. Evidently, the outflows producing these lines are not continuously accelerated from rest along our line of sight. These properties all present challenges for the physical models discussed below.

### Column Densities and Partial Coverage

Estimates of the column densities in each absorbing ion are complicated by the fact that many (most?) intrinsic absorbers only partially cover the background light source(s) along our line(s) of sight. Partial coverage might occur if the absorbing regions are porous or they are smaller than the emission sources in overall projected area (see Fig. 4). In any case, partial coverage leads to unabsorbed flux filling in the bottoms of the measured troughs. The observed line intensities thus depend on both the line-of-sight coverage fraction,  $C_f$ , and the line optical depths as,

$$I_v = (1 - C_f) I_o + C_f I_o e^{-\tau_v} \quad (1)$$

where  $0 \leq C_f \leq 1$ ,  $I_v$  and  $I_o$  are the observed and emitted (unabsorbed) intensities, and  $\tau_v$  is the line optical depth, at each line velocity  $v$ . The first term on the right side represents the unabsorbed light that fills in the troughs. In the limit  $\tau_v \gg 1$  we have simply,

$$C_f = 1 - \frac{I_v}{I_o}$$

Outside of that limit, we can compare lines whose true optical depth ratios are fixed by atomic constants, such as the HI Lyman lines or doublets like CIV  $\lambda\lambda 1548, 1550$ , to determine uniquely both the coverage fractions and the true optical depths across the line profiles. For the commonly measured doublets (like CIV), where the true optical depth ratios are  $\sim 2$ , the coverage fraction at each velocity follows from Eqn. 1 such that,

$$C_f = \frac{I_1^2 - 2I_1 + 1}{I_2 - 2I_1 + 1}$$

where  $I_1$  and  $I_2$  are the observed line intensities, normalized by  $I_o$ , at the same velocity in the weaker and stronger line troughs, respectively. The column densities,  $N$ , follow from the line optical depths via,

$$N = \frac{m_e c}{\pi e^2 f \lambda_o} \int \tau_v dv$$

where  $f$  and  $\lambda_o$  are the line's oscillator strength and laboratory wavelength. The integral is performed over all or part of the line profile.

This analysis has been applied to well-resolved multiplets in NALs and mini-BALs. The derived coverage fractions range from  $\sim 10\%$  to  $100\%$ . The column densities in commonly measured ions (e.g. HI, CIV, NV, SiIV, etc.) are usually in the range  $10^{13} \lesssim N \lesssim 10^{16} \text{ cm}^{-2}$ , consistent with the usual absence of Lyman edge absorption at  $912 \text{ \AA}$ . Most BALs are too broad and blended for this analysis. They probably have  $C_f < 1$  in general, but the exact values are rarely known. Crude estimates suggest that the range of BAL column densities is perhaps an order of magnitude larger than the well-measured NALs.

## Ionization and Total Column Densities

Intrinsic absorbers are in general highly ionized. Their lowest levels of ionization are usually characterized by ions such as CIII, NIII, SiIV or CIV. Lower ionization species like SiII, FeII, MgII or CII are rarely present. The upper limits of ionization are generally not known because higher ions have their resonance lines at shorter (and more difficult-to-measure) wavelengths. Existing data suggest that ionizations up to at least NeVIII are common.

The strong radiative flux of the AGN provides a natural ionization source. Theoretical simulations of photoionized plasmas in equilibrium with the AGN radiation field are used to match the measured column densities, and thus derive the overall ionization state(s) and total column densities (in HI + HII). The ionization state is described by an ionization parameter,  $U$ , which is the dimensionless ratio of hydrogen-ionizing photon to hydrogen particle densities in the absorber:

$$U \equiv \frac{1}{4\pi R^2 c n_H} \int_{\nu_{LL}}^{\infty} \frac{L_\nu}{h\nu} d\nu$$

where  $n_H$  is the absorber's hydrogen density,  $R$  is its radial distance from the central quasar,  $L_\nu$  is the quasar luminosity distribution and  $\nu_{LL}$  is the frequency at the HI Lyman limit. For a "typical" AGN spectral shape we have,

$$U \approx 0.3 n_{10}^{-1} R_{0.1}^{-2} L_{46} \quad (2)$$

where  $n_{10}$  is the density in units of  $10^{10} \text{ cm}^{-3}$ ,  $R_{0.1}$  is the radial distance in units of 0.1 pc, and  $L_{46}$  is the AGN luminosity relative to  $10^{46} \text{ ergs s}^{-1}$ . Typical  $U$  values are between  $\sim 0.01$  and  $\sim 1$ . Absorbers at the same velocity, or at different velocities in the same spectrum, often have a range of  $U$  values implying a range of densities or radii in the overall absorbing region. Derived total column densities are typically  $N_H \approx 10^{19}$  to  $10^{21} \text{ cm}^{-2}$  for NAL regions and  $\gtrsim 10^{22} \text{ cm}^{-2}$  for the BAL gas.

## Correlated X-Ray Absorption

Recent studies have shown that the presence of intrinsic lines in the UV correlates with continuous (bound-free) absorption in soft X-rays. Evidently, the UV lines are just one aspect of the intrinsic absorber phenomenon. The X-ray results are important because they reveal generally higher ionizations,  $U > 1$ , and much higher total column densities, by 1–2 orders of magnitude, compared to the UV lines. A critical issue, therefore, is the physical relationship between the UV and X-ray absorbers.

The data clearly show that different absorbers (of either type) can have a wide range of physical conditions. Some well-measured UV absorbers, in particular, have ionizations and total column densities that

should produce only minimal X-ray absorption. Moreover, the best ensemble data are often inconsistent with a 1-zone medium producing all of the measured features. Spatially distinct zones with different ionizations and column densities are at least sometimes present. It is therefore likely that the UV and X-ray absorbers are physically related but not, in general, identically the same.

## Space Densities and Radial Distances

Most constraints on the radial distance come indirectly from estimates of the space density and ionization parameter (via Eqn. 2). The densities are derived in several ways. For example, the absence of broad or blueshifted forbidden emission lines, e.g. [OIII]  $\lambda 5007$ , suggests (for BAL regions only) that this emission is suppressed by collisional deexcitation at high densities. Some AGNs have absorption lines from excited energy states, implying significant densities to support the upper level populations. In other cases, time-variable absorption lines require minimum densities to allow the gas to adjust its ionization structure within the variability time. This last method assumes that the variability time exceeds the recombination time,  $t_{recomb} \approx (n_e \alpha)^{-1}$ , where  $n_e$  is the electron density and  $\alpha$  is the recombination rate coefficient. Even if the line variability is not caused by changes in the ionization, it turns out that dynamical limits on clouds moving across our line of sight lead to similar  $R$  constraints.

The overall results imply densities from  $\lesssim 7 \text{ cm}^{-3}$  to  $> 10^6 \text{ cm}^{-3}$  and corresponding distances from  $\gtrsim 300 \text{ kpc}$  to  $\lesssim 10 \text{ pc}$  in different sources. The largest confirmed distances apply only to narrow and non-variable NALs. Lines with clear dynamic signatures, e.g. the BALs, mini-BALs and some NALs, probably form closer to the AGN than even the smallest of these upper limits. The minimum radial distance,  $R_{min}$ , is set by the fact that many intrinsic absorbers, e.g. most BALs, suppress both the continuum and broad line emissions. The absorber distances therefore cannot be much less than the broad emission line region radius, which is known independently to scale with the AGN luminosity, such that,

$$R_{min} \approx 0.1 (L_{46})^{\frac{1}{2}} \text{ pc} \quad (3)$$

where  $L_{46} \approx 1$  is "typical" for quasars. (Values of  $L_{46}$  can actually range from  $\lesssim 0.001$  in Seyfert nuclei to  $> 100$  in the most luminous quasars.) If there is absorbing gas near this minimum radius, the densities could reach  $\sim 10^{10} \text{ cm}^{-3}$  (see Eqn. 2).

## Physical Models

Most physical models of intrinsic absorbers feature a wind-disk geometry similar to Fig. 4. The outflowing gas stays close to the accretion-disk plane, and we

observe it (via blueshifted absorption lines) only if our sight line(s) to the emission source(s) intersect wind material. The disk provides a likely source for the wind material, and its acceleration to high speeds probably occurs via radiation pressure from the central emission source. The outward transfer of angular momentum in these winds might facilitate the *inward* flow of matter in the accretion disk, thus promoting the growth and fueling of the central black hole.

The measured line velocities suggest that the outflows often originate near the minimum radius implied by Eqn. 3. In particular, the radial acceleration of a wind driven by radiation pressure from a central point source with luminosity  $L$  and mass  $M$  is,

$$\frac{v dv}{dR} = \frac{f_L L}{4\pi R^2 c m_H N_H} - \frac{GM}{R^2}$$

where  $f_L$  is the fraction of the luminosity absorbed or scattered in the wind. Integrating this equation from  $R$  to infinity yields the terminal velocity,

$$v_\infty \approx 10,000 R_{0.1}^{-\frac{1}{2}} \left( \frac{f_{0.1} L_{46}}{N_{22}} - 0.8 M_9 \right)^{\frac{1}{2}} \text{ km s}^{-1} \quad (4)$$

where  $N_{22}$  is the total column density in  $10^{22} \text{ cm}^{-2}$ ,  $M_9$  is the central black hole mass relative to  $10^9 M_\odot$ , and  $f_{0.1}$  is the absorbed fraction compared to 10%. These expressions hold strictly for open geometries, where the photons escaping one location in the wind are not scattered or absorbed in another location. Estimates of the total absorption indicate that  $f_{0.1}$  could be as large as a few for BAL flows, and proportionately less for the narrower mini-BALs and NALs. Estimates of  $N_{22}$  range from  $\lesssim 0.01$  for some intrinsic NALs to  $\gtrsim 1$  for typical BALs. Radiative acceleration therefore requires small radii — very roughly similar to the radius of the broad emission line region.

The radial scale is important for defining the mass and kinetic energy of outflowing gas. The total wind mass at any instant is,

$$M_w \approx 1.1 Q_{0.1} N_{22} R_{0.1}^2 M_\odot$$

where  $Q_{0.1}$  is the global covering factor relative to 10%. The mass loss rate,  $\dot{M}_w$ , depends further on the characteristic flow time,  $v/\Delta R$ , such that,

$$\dot{M}_w \approx 0.11 Q_{0.1} N_{22} \frac{R_{0.1}^2}{\Delta R_{0.1}} v_4 M_\odot \text{ yr}^{-1}$$

where  $v_4$  is the flow velocity in units of  $10^4 \text{ km s}^{-1}$  and  $\Delta R_{0.1}$  is its radial thickness in units of 0.1 pc. The kinetic energy luminosity is  $L_K \approx \frac{1}{2} \dot{M}_w v^2$ , or,

$$L_K \approx 4 \times 10^{42} Q_{0.1} N_{22} \frac{R_{0.1}^2}{\Delta R_{0.1}} v_4^3 \text{ ergs s}^{-1}$$

During a quasar's lifetime, perhaps  $\sim 10^8$  yrs, outflows with these parameter values will eject a total of  $\sim 10^7 M_\odot$  of gas with kinetic energy  $\sim 10^{58}$  ergs. BAL winds might often have total masses, kinetic energies, etc., that are an order of magnitude larger, based on our best estimates of  $Q_{0.1} \approx 1-3$  and  $N_{22} \gtrsim 1$  for those outflows.

One unresolved issue is whether the outflowing gas is smoothly distributed or residing in discrete clouds. This seemingly simple question goes to the heart of the wind physics. It was long believed that the flows consist of many discrete clouds because, for example, a flow with  $N_{22} \approx 1$  and  $\Delta R_{0.1} \approx R_{0.1} \approx 1$  would have a mean density of only  $n \approx 3 \times 10^4 \text{ cm}^{-3}$ . This density would lead to  $U$  values several orders of magnitude larger than expected from the data (Eqn. 2). Moreover, a gas with this high ionization cannot be radiatively accelerated because the ions would be too stripped of electrons to absorb enough incident flux. The flows must therefore be distributed in much denser clouds that fill only part of the wind volume. If these clouds individually have velocity dispersions close to the sound/thermal speed (roughly  $15 \text{ km s}^{-1}$  for a nominal 15,000 K gas), then a smooth BAL profile of width  $10^4 \text{ km s}^{-1}$  requires  $\gtrsim 1000$  clouds along the line of sight. The main objection to this scenario is that the clouds must be very small,  $\lesssim 10^9$  cm across, and they cannot survive as discrete entities without some ad hoc external pressure.

An alternative model has emerged in which the flows are, in fact, smoothly distributed with high ionization parameters. The high  $U$  values,  $\gtrsim 100$ , are reconciled with the data (and with radiative acceleration) by invoking a large column density ( $N_H \gtrsim 10^{23} \text{ cm}^{-2}$  for BAL winds) of highly ionized gas at the base of the flow. This gas is not radiatively accelerated because it is too ionized. But its bound-free absorption (in soft X-rays and the extreme UV) greatly "softens" the spectrum seen by the wind material downstream, thereby lowering the wind's ionization level and facilitating its acceleration. The most compelling aspect of this model is that it provides a physical basis for the observed correlation between UV and X-ray absorption: the winds revealed by the UV lines cannot exist without the shielding X-ray absorber. The leading alternative explanation, which simply equates the 2 absorbing regions, presents a serious problem because the high column densities implied by the X-ray absorption might be impossible to radiatively accelerate (Eqn. 4).

A serious challenge to all models is the kinematic complexity. It is surprising, for example, that no intrinsic absorbers have shown line-of-sight acceleration. The crossing time for a flow with  $v_4 = 2$  and  $\Delta R_{0.1} = 1$  is only  $\sim 5$  yrs, yet repeated observations over this time frame reveal no velocity changes. Just as challenging are the multi-component line troughs and the frequent lack of absorption near zero velocity. These characteris-

tics might be caused by the episodic ejection of discrete “blobs,” or by well-collimated flows that cross our line of sight and thus reveal only part of their full velocity extent. The latter hypothesis seems more likely for at least the broader lines, because their super-sonic velocity dispersions ( $>1000 \text{ km s}^{-1}$ ) should quickly dissipate discrete blobs. Collimated accretion disk winds might cross our line of sight if they are driven at first vertically off the disk, before being bent into fully radial motion by the AGN’s radiative force. The collimation and vertical ejection might both be facilitated by magnetic fields running perpendicular through the disk plane. However, multiple line troughs would require multiple collimated outflows. A major problem with this picture is that these intricate flow structures, which are tied to the accretion disk, must remain stable while the disk rotates.

A more general problem is determining how much, and what aspects, of the diversity among intrinsic absorbers results simply from orientation effects. Do the various outflows identified by BALs, mini-BALs and intrinsic NALs coexist generally in AGNs? Orientation is clearly not the only factor. For example, the complete lack of high-velocity lines in Seyfert galaxies suggests a luminosity dependence, probably related to the requirements for radiative acceleration. Similarly, the relationships to AGN radio emissions suggest that there is some (unknown) physical connection between the disk-wind properties and the formation of radio jets.

## Element Abundances and Host Galaxy Evolution

Our understanding of the element abundances near AGNs is based on general principles of stellar nucleosynthesis and galactic chemical evolution. All of the heavy elements from carbon on up are synthesized from primordial H and He in stars. The amounts of these elements are thus revealing of both the amount of local star formation and the evolutionary status of the galactic environment. The elements near AGNs specifically probe these properties in the centers of big galaxies. For distant quasars, the local abundance evolution might involve some of the first stars forming in collapsed structures after the Big Bang.

Abundance measurements from absorption lines are, in principle, quite simple; one has only to apply appropriate correction factors for the ionization to convert the ionic column densities into relative abundances. For example, the abundance ratio of any two elements  $a$  and  $b$  can be written simply as,

$$\frac{a}{b} = \frac{N(a_i) F(b_j)}{N(b_j) F(a_i)}$$

where  $N$  and  $F$  are respectively the column densities and number fractions of element  $a$  in ion state  $i$ , etc., in

the absorbing gas. The  $F$  values are generally adopted from photoionization calculations.

The results from intrinsic NALs, and independently from the broad emission lines, indicate that quasar environments have roughly solar or higher heavy-element abundances out to redshifts  $>4$ . (Results based on the BALs are so far unreliable because of the problems with partial line-of-sight coverage mentioned earlier.) The local star formation must be both rapid and extensive to achieve these high abundances at early cosmic times. In particular, much of the gas must have already collapsed into stars by the time the quasars “turned on” or became observable — just a few billion years after the Big Bang. These findings support prior expectations for the rapid, early-epoch evolution of massive galactic nuclei.

## Bibliography

Studies of intrinsic AGN absorption lines began in the 1960s with measurements of BALs and associated NALs in quasars. The status of the field circa 1997 is summarized in numerous articles and reviews in the conference proceedings, Arav A, Shlosman I and Weymann R J (eds.) *Mass Ejection from AGN* (ASP Conference Series: San Francisco). More recent results on the BALs appear, with further references, in Hamann F 1998 Broad PV Absorption in the QSO PG 1254+047: Column Densities, Ionizations and Metal Abundances in Broad Absorption Line Winds *Astrophys. J.* **500** 798–809. The latest results on intrinsic X-ray absorption are discussed by Brandt W N, Laor A, & Wills B J 1999 On the Nature of Soft X-Ray Weak Quasi-Stellar Objects *Astrophys. J.* **528** 637. The status of the polarization work on BAL quasars is described by Schmidt G D & Hines D C 1999 The Polarization of Broad Absorption Line QSOs *Astrophys. J.* **512** 125, and by Ogle P M, et al. 1999 Polarization of Broad Absorption Line QSOs. I. A Spectropolarimetric Atlas *Astrophys. J. Suppl.* **125** 1–34. A recent summary of intrinsic UV absorption in Seyfert galaxies appears in Crenshaw D M, Kraemer S B, Boggess A, Maran S P, Mushotzky R F, & Wu C-C 1999 Intrinsic Absorption Lines in Seyfert 1 Galaxies: I. Ultraviolet Spectra from the Hubble Space Telescope *Astrophys. J.* **516** 750–768. The work on AGN element abundances is reviewed by Hamann F H & Ferland G J 1999 Elemental Abundances in QSOs: Star Formation and Galactic Nuclear Evolution at High Redshifts *Ann. Rev. Astr. Astrophys.* **37** 487.

## Author’s Credit

Frederick Hamann  
University of Florida